UNIVERSITY OF NOTRE DAME

Computationally Determining Stationary States for 1-Dimensional Potentials

Isaiah Mumaw

March 28, 2021

1 BACKGROUND

One of the most fundamental discoveries of quantum mechanics is the Schrödinger equation, a linear partial differential equation which governs the evolution of a wave function over time. In its most general form, it is given as:

$$i\hbar\frac{\partial}{\partial t}|\Psi(t)\rangle = \hat{H}|\Psi(t)\rangle \tag{1.1}$$

The Hamiltonian operator, $\hat{H}$, is then defined as the sum of kinetic and potential energy contributions. In one-dimensional position space, this is given as:

$$\hat{H} \equiv -\frac{\hbar^2}{2m}\frac{\partial^2}{\partial^2 x} + V(x,t) \tag{1.2}$$

For cases where the potential energy function does not change with time, we can separate the wave function into space and time components: $\Psi(x,t) = \psi(x)\varphi(t)$. This allows Eq. 1.1 to be solved through separation of variables. For the space component, we get:

$$\hat{H}|\psi\rangle = E|\psi\rangle \tag{1.3}$$

The resulting set of solutions, $|\psi_n\rangle$, gives the eigenstates of $\hat{H}$, with eigenvectors E_n representing the energy of each state.

By the same process, the time component is then given by the following:

$$|\varphi_n\rangle = e^{-iE_n t/\hbar} \tag{1.4}$$

Recombining these solutions into $|\Psi_n(t)\rangle$ gives a set of stationary states, as the complex square removes time dependence and thus gives a constant probability density over time.

These states also create a complete orthonormal basis, such that any wave function can be written as a linear combination of stationary states:

$$|\Psi(t)\rangle = \sum_n^\infty c_n e^{-iE_n t/\hbar} |\psi\rangle \tag{1.5}$$

Therefore, in order to predict the behavior of any particle in a given potential, one must first find the stationary states of that potential.

2 Solution using Linear Combinations

The first iteration of the code was built around the methods taught in introductory quantum mechanics. Starting with a set of basis states and a potential energy function, we populated the Hamiltonian matrix. Using this matrix, we then found the appropriate linear combination of states for each energy level in the potential energy function.

2.1 Stationary States

Many realistic situations can be approximated by the quantum harmonic oscillator, making it a good choice for a basis. It has a potential energy function given by:

$$V(x) = \frac{1}{2} m\omega^2 x^2 \tag{2.1}$$

with the following stationary states, where $H_n(\xi)$ is a Hermite polynomial of degree n, and $\xi \equiv \sqrt{\frac{m\omega}{\hbar}} x$:

$$|\psi_n\rangle = \left(\frac{m\omega}{\pi\hbar}\right)^{1/4} \frac{1}{\sqrt{2^n n!}} H_n(\xi) e^{-\xi^2/2} \tag{2.2}$$

Because numpy is vectorized, the wave function can be easily calculated over a large array of points. For the purposes of this report, we will be using the following units: $m = \omega = \hbar = 1$, and π taking its established value up to 16 significant figures.

2.2 Populating the Hamiltonian

The bulk of the code is centered around populating the Hamiltonian matrix. The elements of the matrix are given such that they satisfy Eq. 1.3:

$$H_{ij} = \langle \psi_i | \hat{H} | \psi_j \rangle = \int \psi_i^*(x) \left(-\frac{\hbar^2}{2m} \frac{\partial^2}{\partial^2 x} + V(x) \right) \psi_j(x) dx \tag{2.3}$$

This action is performed computationally by separately finding the kinetic and potential portions of the integral, and adding them together at the end. The kinetic portion used numpy.gradient() twice in order to get the second derivative, and both parts of the integral were calculated using Simpson's Rule, which is built into the scipy.integration module. Simson's rule was chosen because it has a low error value compared to trapezoidal and midpoint rules. The integration will be performed over the region of non-negligible probability.

The operation is then repeated over a square matrix of dimension $N \times N$. While technically the true Hamiltonian is infinite, a finite approximation works, so long as the levels being analyzed, n, are much smaller than N.

2.3 Diagonalization

The next step is to diagonalize the Hamiltonian matrix. This was done using the function numpy.linalg.eigh(), which returns the eigenvalues and eigenvectors, sorted from the lowest to highest eigenvalue. The diagonal matrix is then filled out using the eigenvalues:

$$\begin{vmatrix} E_0 & 0 & \cdots & 0 \\ 0 & E_1 & \cdots & 0 \\ \vdots & \vdots & \ddots & \vdots \\ 0 & 0 & \dots & E_{N-1} \end{vmatrix} \tag{2.4}$$

The associated eigenvectors can then be plugged into Eq. 1.5 as the values for c_n, thus giving the stationary states for the potential.

2.4 Analysis of Correctness

As a test of accuracy, the code was executed using the harmonic oscillator potential from Eq. 2.1. Given a large enough Hamiltonian, the energies should converge on the following:

$$E_n = \hbar\omega \left(n + \frac{1}{2} \right) \tag{2.5}$$

This is exactly the behavior observed. The first ten energy levels are shown in Figure 2.1. Because we are using the same potential used to derive the basis states, the energies converge almost immediately. Figure 2.2 shows the calculated energies compared to the known energies, as given in Eq. 2.1.

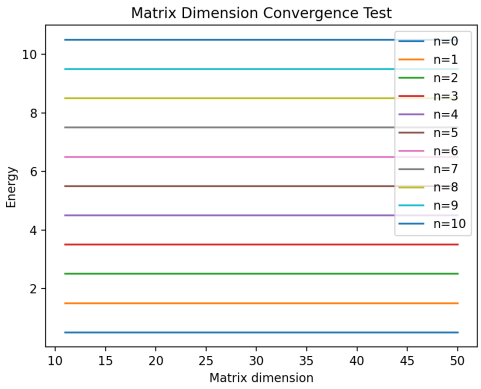

Figure 2.1

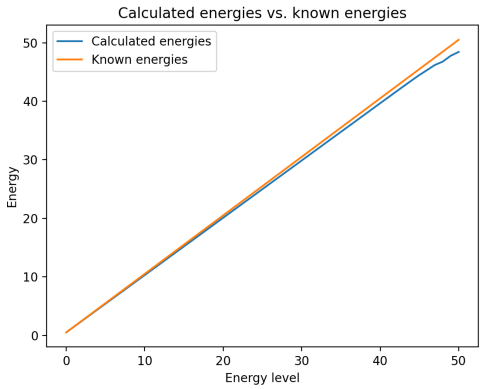

Figure 2.2

The stationary states should also be unchanged from the original harmonic oscillator equation, which is the exact behavior observed. Figures 2.3 and 2.4 show the known and calculated wave function probabilities for the ground state and 15th excited state. Note that the calculated ground state perfectly overlaps the known state, and there are only minor deviations for the excited state.

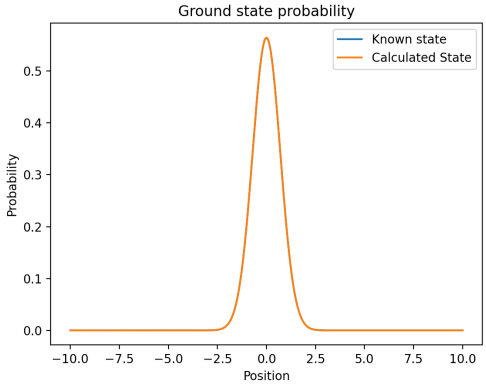

Figure 2.3

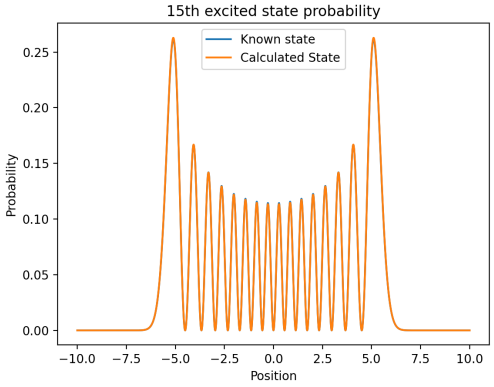

Figure 2.4

The raw wave functions were also very similar to the established wave functions, though the some states had inverted amplitudes despite having identical probability distributions, as shown in Figures 2.5 and 2.6.

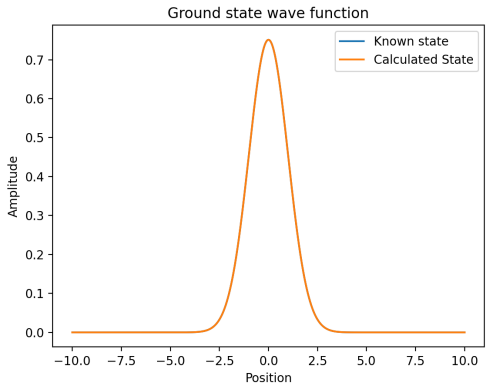

Figure 2.5

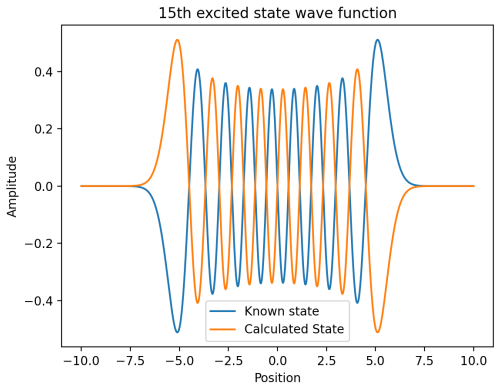

Figure 2.6

3 Algorithmic solution

While the linear combination method provides an intuitive, step-by-step process of solving the Schrödinger equation, it is also very processor-heavy for matrices larger than $N = 50$. However, in his published lectures, Dr. Hjorth-Jensen proposes a much more elegant solution using Lanczos' algorithm.

3.1 Deriving and Generating the Matrix

If we write Eq. 1.3 in full and set all constants to 1 (as before), we get the following:

$$-\frac{d^2}{dx^2}\psi(x) + V(x)\psi(x) = 2E\psi(x) \tag{3.1}$$

To get the second derivative discretely, we take an array of equally-spaced x values with length N, ranging from x_{min} to x_{max}. The step size, h, is given as:

$$h = \frac{x_{max} - x_{min}}{N} \tag{3.2}$$

With x now discretized, the second derivative of any function can be found using the following formula:

$$\frac{d^2}{dx^2}f(x) = \frac{f(x+h) - 2f(x) + f(x-h)}{h^2} \tag{3.3}$$

Now, if we define an arbitrary x value in the array as:

$$x_k = x_{min} + kh \qquad\qquad k = 1, 2, \ldots, N-1 \tag{3.4}$$

then we can use the above equations to rewrite Eq. 3.1 at any point x_k as:

$$\frac{\psi(x_{k+1}) - 2\psi(x_k) + \psi(x_{k-1})}{h^2} + V(x_k)\psi(x_k) = 2E\psi(x_k) \tag{3.5}$$

Now, for symmetric eigenvalue problems, we can apply Lanczos' algorithm to get a fairly good estimate of the solution. This algorithm creates a very large tridiagonal matrix, which for this case has diagonal elements:

$$d_k = \frac{2}{h^2} + V(x_k) \tag{3.6}$$

and off-diagonal elements:

$$e_k = -\frac{1}{h^2} \tag{3.7}$$

Due to the factor of 2 attached to E in Eq. 3.1, the resulting eigenvalues must be divided by 2 in order to get the correct energy values. The eigenvectors of the matrix are the wave functions at each energy level, though they must be normalized to get appropriate results [2].

The matrix is generated using Eqs. 3.6 and 3.7, first at the corners, then by looping through the non-zero elements inside the corners. The eigenvalues and eigenvectors are found using a similar function as in the previous section, though with the appropriate corrections as discussed above.

3.2 Analysis of Correctness

As before, we can use the harmonic oscillator states as a test case. The energies should again converge according to Eq. 2.5. However, instead of just adjusting the maximum energy level of the matrix, we can adjust both the step size and range of values for x. Figures 3.1 and 3.2 show the convergence of energies, controlling for both of these factors.

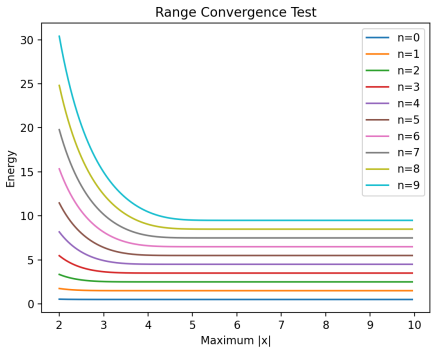

Figure 3.1: $|x|_{max}$ varies from 2 to 10, $h = .05$

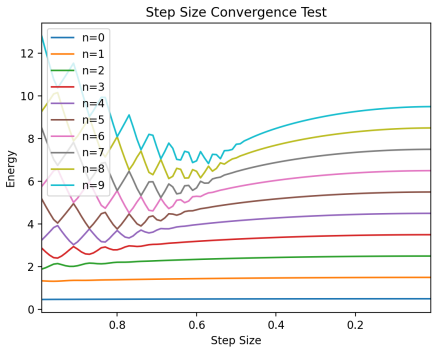

Figure 3.2: h varies from 1 to .05, $|x|_{max} = 10$

Given that the energies converge, they can now be compared to Eq. 2.5, as shown in Figure 3.3. For lower energies, this method is very accurate, however the calculation breaks down for higher energy levels. Based on the results, it also appears that increasing the range has a far greater effect than decreasing the step size.

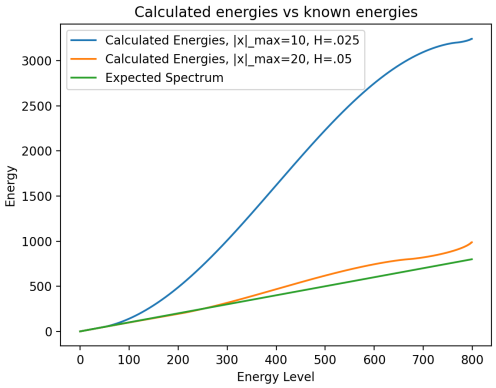

Figure 3.3

And as before, the stationary states are largely unchanged. This method is even more precise than the first method, so there is negligible deviation even for higher energy levels. Figures 3.4 and 3.5 show the probabilities for ground state and 15th excited state. As with the previous method, it did invert some of the amplitudes of the raw wave function, but had no effect on the probability (not shown, as the effect is identical).

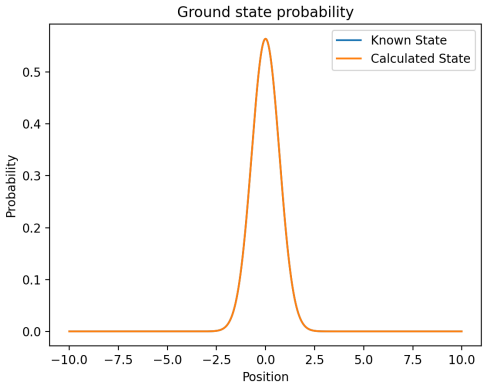

Figure 3.4

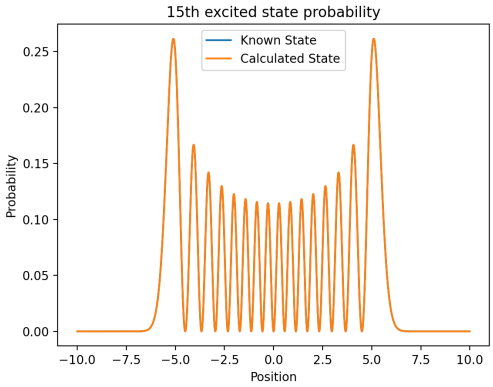

Figure 3.5

‘

4 Application to new potentials

With the accuracy established, we then applied our methods onto two new potential energy functions.

4.1 Quartic Perturbation to Harmonic Potential

Perturbation theory is a procedure used to obtain approximate solutions for a potential energy function. Specifically, the potential must be a combination of a known potential and a small adjustment [1]. In this case, we chose a potential of the form:

$$V(x) = \frac{1}{2}m\omega^2 x^2 + \epsilon x^4 \tag{4.1}$$

where $\epsilon << \frac{1}{2}m\omega^2$. The resulting energies and stationary states should be very similar to those of the harmonic oscillator, with proportionally greater deviations from the unperturbed states at higher energy levels.

First, we set $\epsilon = 0.1$. For the linear combination method, the energies converged according to Figure 4.1. For the algorithmic method, the energies converged according to Figs. 4.2 and 4.3 (next page). The behavior of both methods matched expectations, with lower energies being closer together and more similar to the unperturbed state than higher energies.

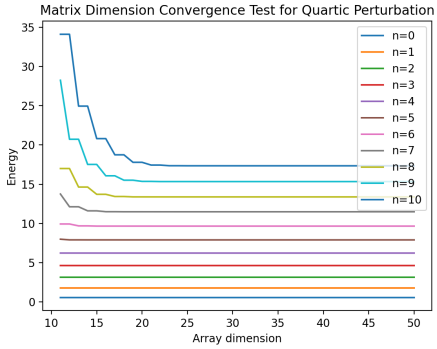

Figure 4.1: Calculated using step size .01, with $-10 \leq x \leq 10$

The resulting energy values for each method agreed with each other. Figure 4.4 plots the results of both methods, as well as the results for perturbation theory (up to second order corrections), and the unperturbed energies. As already shown by the convergence tests, the differences in energy between perturbed and unperturbed states increases with each subsequent energy level. This plot also shows the shortcomings of perturbation theory at higher energy levels.

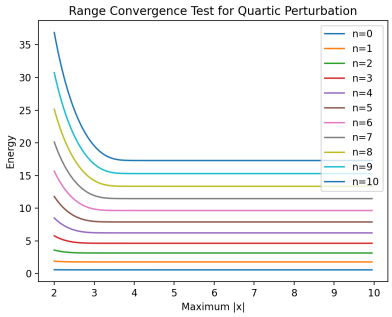

Figure 4.2: Calculated with $h = .05$

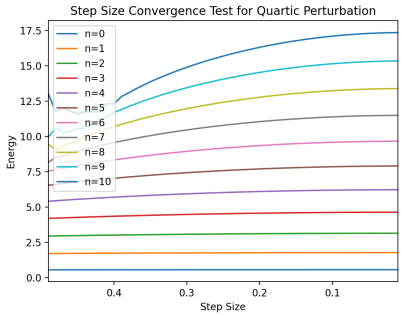

Figure 4.3: Calculated with $|x| = 10$

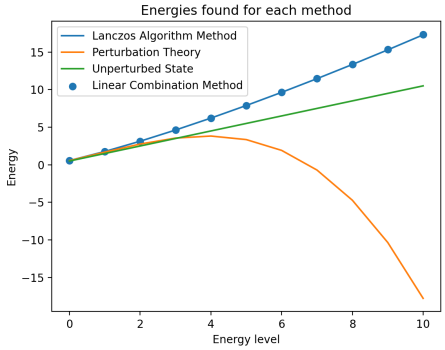

Figure 4.4

The resulting stationary states for each method roughly matched expectations, with the probability peaks, shown in Figure 4.5, becoming sharper and narrower than the unperturbed state because the particle is confined to a steeper well. The ground state and the state $n = 3$ are shown in Figure 4.6, alongside the corresponding unperturbed state. Both methods produced almost identical plots.

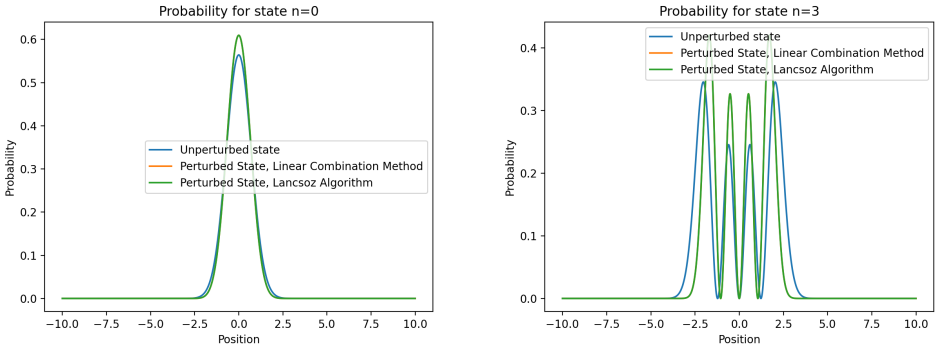

Figure 4.5

The same inversion of amplitude did occur in this plots, though again only for higher energy levels.

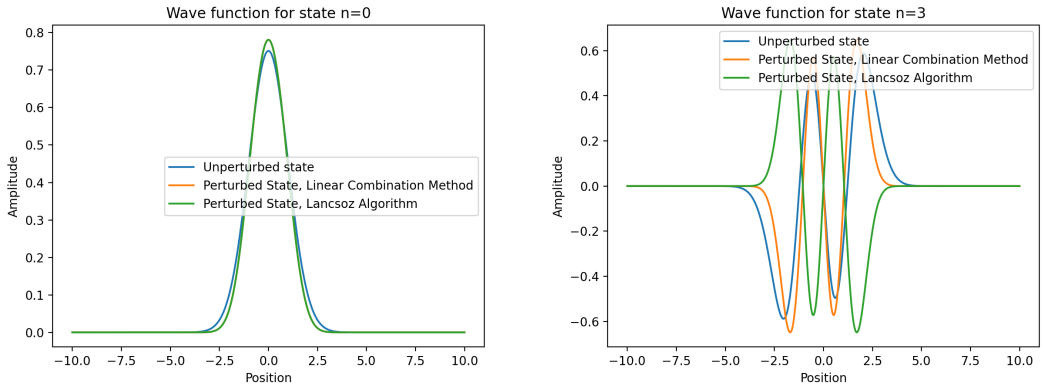

Figure 4.6

This process was repeated for the case where $\epsilon = 0.5$. In this case, the perturbation is large compared to the original potential.

Figure 4.7 shows the convergence for the linear combination method, and Figures 4.8 and 4.9 show the convergence for the algorithmic method. Convergence took longer in most cases (except for the range convergence), but still converged within the bounds of the test.

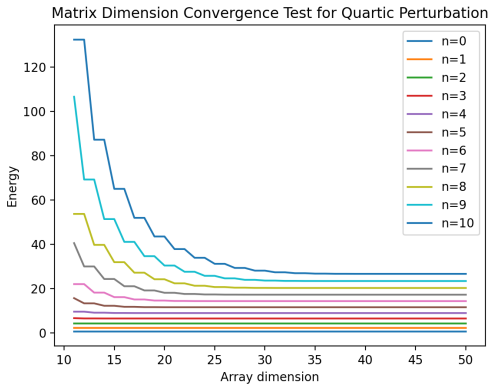

Figure 4.7: Calculated using step size .01, with $-10 \leq x \leq 10$

The resulting energy values for each method agreed with each other. Figure 4.10 plots the calculated energies, as well as unperturbed energies and the energies calculated from perturbation theory. In this case, perturbation theory fails almost immediately, as the perturbation is far too large.

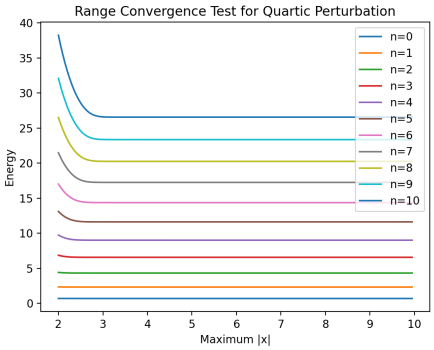

Figure 4.8: Calculated with $h = .05$

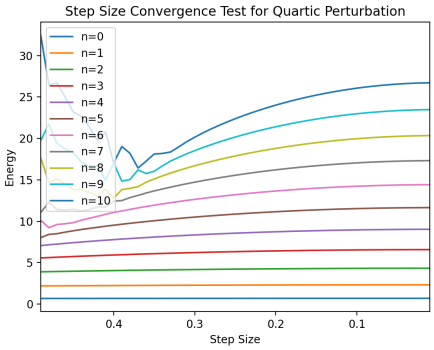

Figure 4.9: Calculated with $|x| = 10$

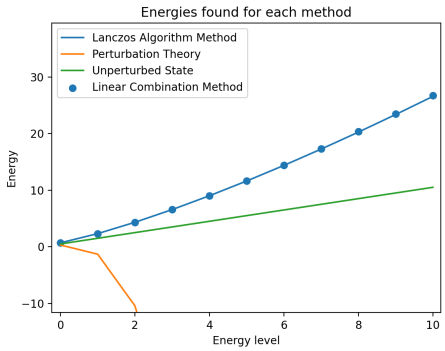

Figure 4.10

The resulting stationary states for each method also matched expectations, closely resembling those from before, but with even more tightly constrained peaks. The ground state and the state n=3 are shown in Figure 4.11. As before, both methods produced identical results. They also had identical issues with the amplitudes for the raw wave function.

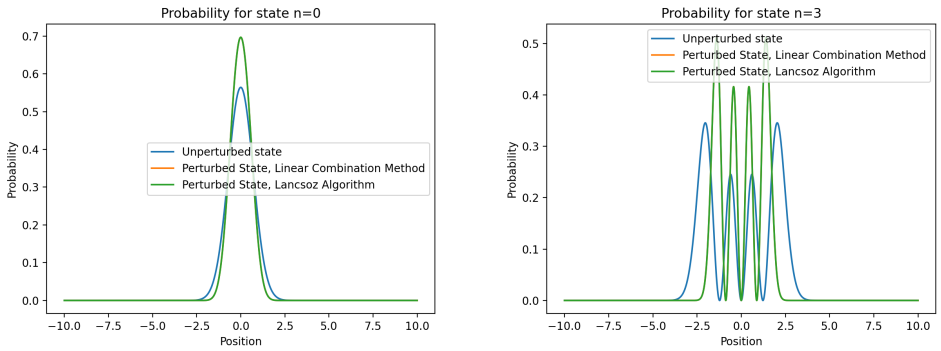

Figure 4.11

4.2 Double Harmonic Well Potential

The second potential we analyzed was the double harmonic well, which resembles two adjacent harmonic oscillator potentials. It has a potential energy function given by the following, where E_0 and C are constants:

$$V(x) = E_0(Cx^4 - x^2) \tag{4.2}$$

For this section, we have set $E_0 = 1$ and $C = 0.05$, shown in Figure 4.12.

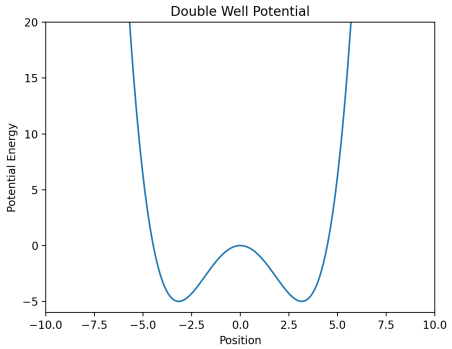

Figure 4.12

For the linear combination method, the energies converged according to Figure 4.13. For the algorithmic method, the energies converged according to Figures 4.14 and 4.15. Of note is that the energies pair together at the lower energy levels, implying that the wave functions of each pair are very similar. Pairing behavior seems to quickly taper off as energies exceed 0, starting with the state $n = 6$, where the energy is great enough that the double well begins to resemble a single well.

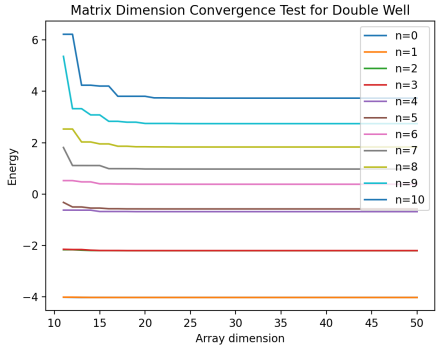

Figure 4.13

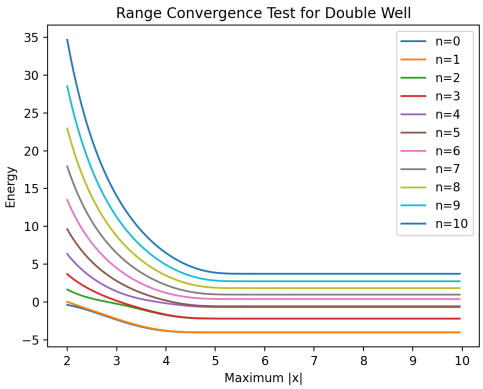

Figure 4.14: Calculated with $h = .05$

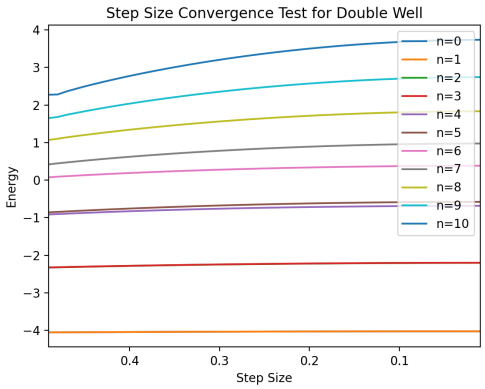

Figure 4.15: Calculated with $|x| = 10$

The resulting energies agree with each other, as shown in Figure 4.16. This figure also shows the pairing effect more clearly.

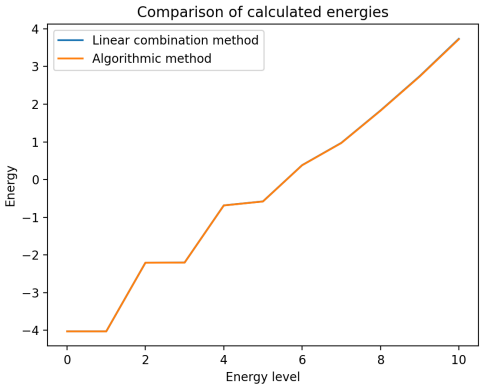

Figure 4.16

The resulting stationary states for each method matched the expectations from the energy spectrum. Lower energy states, shown in Figure 4.17, have probability distributions that are almost identical. Higher energy states do not have the same effect, as shown in Figure 4.18, though there is similar behavior between odd- and even-numbered energy levels.

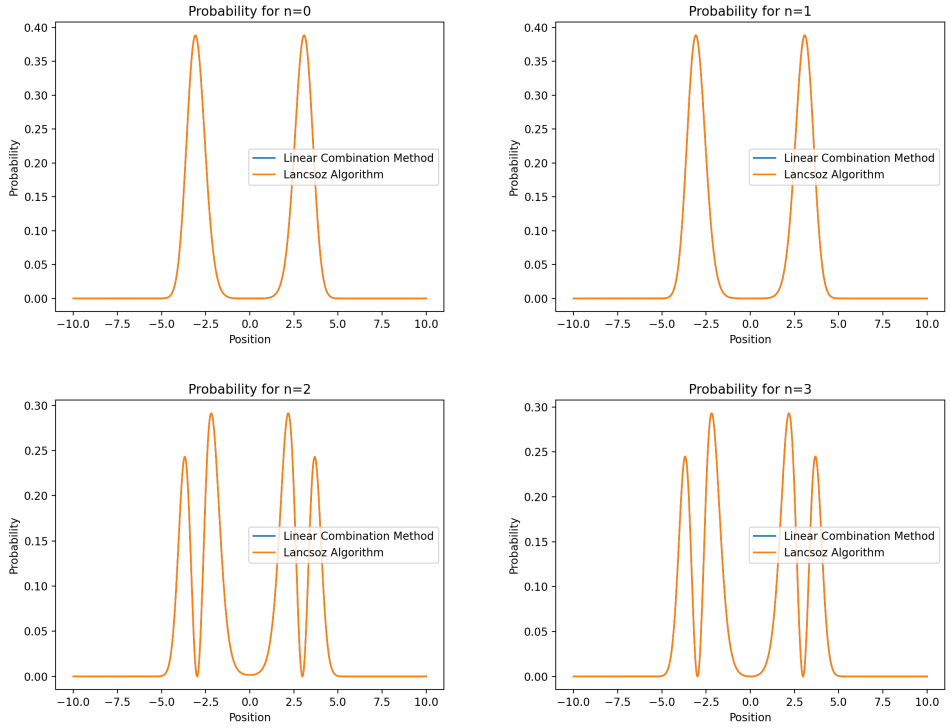
Probability for n=0
Probability for n=1
Probability for n=2
Probability for n=3
Linear Combination Method
Lancsoz Algorithm
Probability
Position

Figure 4.17

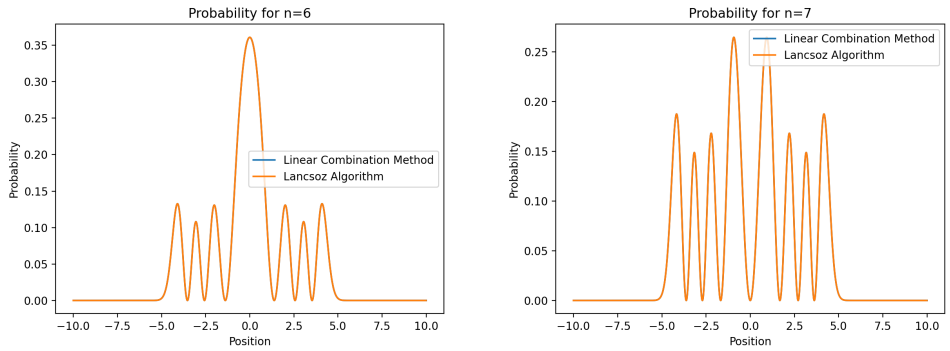
Probability for n=6
Probability for n=7
Linear Combination Method
Lancsoz Algorithm
Probability
Position

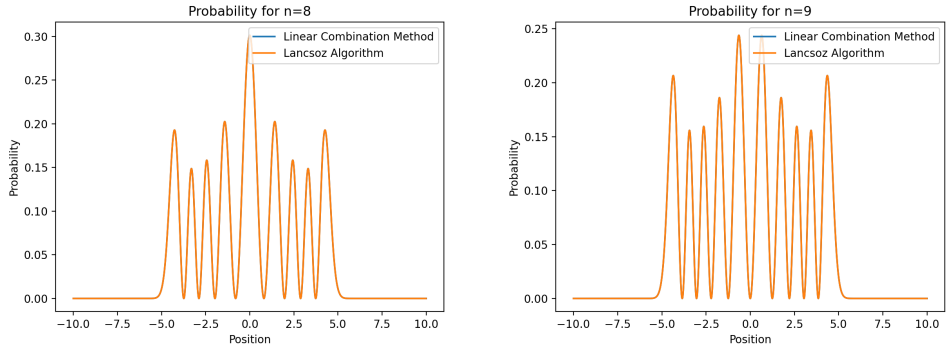

Figure 4.18

However, despite having nearly identical probability distributions, the paired low-energy states do have different wave functions. In particular, odd-numbered wave functions are odd functions, and vice versa, as shown in Figure 4.19. There are some phase issues between the two methods as before, but again this has no bearing on the final probability or energy, which are the primary focus here.

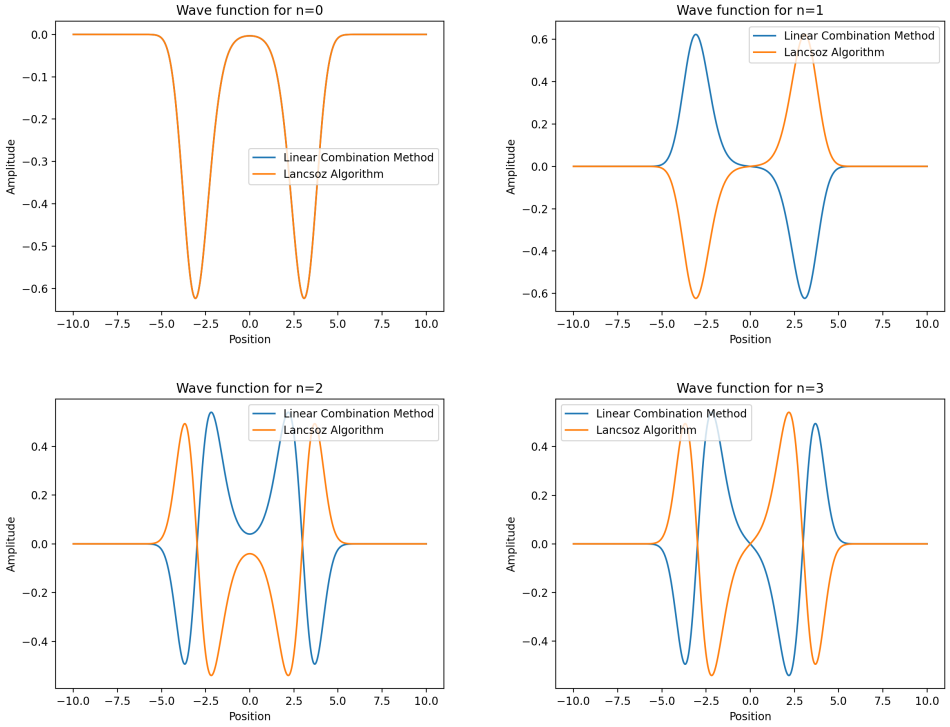

Figure 4.19

5 Discussion

The results obtained in this report demonstrate the importance of computational methods to the field of quantum mechanics. These results also reaffirm known behaviors of particles in potentials with known solutions, and demonstrate the behaviors of particles in potentials that do not have easily derived solutions.

Future iterations of this code will likely need to account for more realistic potentials in two or three dimensions, perhaps beginning with the hydrogen atom. While further improvements may be made to the already existing code, the current iteration is already highly optimized, and many of its limitations are due to the machine it is running on.

The applications of the methods in this code are widespread. Given any one-dimensional potential, it has the ability to produce hundreds of stationary states very rapidly, and if the modifications mentioned above are implemented, is may be able to produce accurate results for almost any situation with a known potential function.

References

[1] Griffiths, D., & Schroeter, D. (2018). *Introduction to Quantum Mechanics (3rd ed.)*. Cambridge: Cambridge University Press.

[2] Hjorth-Jensen, M. (2015). *Computational Physics: Lecture Notes Fall 2015*. University of Oslo.